Weak coupling and dipole bands in ^{191}Pb

N. Fotiades,[1] J. A. Cizewski,[1] D. P. McNabb,[1] K. Y. Ding,[1] D. E. Archer,[2] J. A. Becker,[2] L. A. Bernstein,[2] K. Hauschild,[2] W. Younes,[2] R. M. Clark,[3] P. Fallon,[3] I. Y. Lee,[3] A. O. Macchiavelli,[3] and R. W. MacLeod[3]

[1]*Department of Physics and Astronomy, Rutgers University, New Brunswick, New Jersey 08903*

[2]*Lawrence Livermore National Laboratory, Livermore, California 94550*

[3]*Nuclear Science Division, Lawrence Berkeley National Laboratory, Berkeley, California 94720*

(Received 10 November 1997)

Excited states in the nucleus ^{191}Pb have been investigated by in-beam γ-ray spectroscopic techniques using the Gammasphere array. The reaction ^{173}Yb(^{24}Mg,6n) at a beam energy of 134.5 MeV was used to populate states of ^{191}Pb. The level scheme of ^{191}Pb has been extended up to 5.1 MeV excitation energy and spin 45/2. The lower part (below $\approx$2.3 MeV) presents the general features common in all odd-mass Pb isotopes, i.e., spherical states built on the $13/2^+$ isomer, with bandlike structures that follow weak-coupling expectations. In the upper part of the level scheme two dipole bands are observed with bandhead energies of $\sim$2.512 and 2.291 MeV. A comparison of dipole band 1 with the strongest negative-parity dipole bands in the heavier odd-mass Pb isotopes reveals striking similarities. The spherical states are interpreted as the coupling of the $i_{13/2}$ neutron hole to the yrast states in the even-mass ^{192}Pb core. The dipole bands are interpreted as $M1$ cascades which arise from the coupling of two protons in high-j orbitals above the $Z=82$ gap to neutron holes in the $i_{13/2}$ orbital. [S0556-2813(98)02504-7]

PACS number(s): 23.20.Lv, 23.20.En, 27.80.+w

I. INTRODUCTION

The excitations of the $N\approx114$ lead isotopes show a wide variety of structures. At low angular momentum, the structure is dominated by a single neutron coupled to the weakly collective, spherical even-A cores. At higher spins, cascades of dipole transitions with single-particle $M1$ strengths, but weak $E2$ strengths, have been observed in more than 20 isotopes in this mass region [1–29]. Proton particles in the $h_{9/2}$ and $i_{13/2}$ orbitals coupled to $i_{13/2}$ neutron holes at small oblate deformations have been invoked for their interpretation. The tilted axis cranking (TAC) model [30] describes successfully the coupling between these orbitals with the rotation of the core to reproduce the increasing of spin within a band and the strength of the $M1$ transitions. The regular energy spacings of these dipole bands are expected to become less regular as the quadrupole collectivity increases. Finally, at high angular momenta superdeformed bands become yrast [31].

In this paper the first extensive level scheme of ^{191}Pb built upon the $13/2^+$ isomer is reported. While there are only preliminary reports available on ^{189,190}Pb [32], the heavier odd-mass Pb isotopes have been extensively studied [1–10]. The spectroscopy of ^{191}Pb has been published only in the work reported in [33], where four intense transitions in ^{191}Pb were observed and the first three positive-parity states and one negative-parity state above the $13/2^+$ isomer were deduced.

In the present work 63 transitions were identified and placed connecting 47 levels in ^{191}Pb. Four of these transitions were also reported in [33], and their assignment confirmed. Spin and parity assignments for many of these new levels were possible. A strongly populated dipole band, of assumed $M1$ character, has been observed. The properties of this level scheme, and in particular of the dipole bands, are compared with those observed in the heavier Pb isotopes.

II. EXPERIMENT

The ^{173}Yb(^{24}Mg,6n) reaction was used to populate excited states of ^{191}Pb with a beam energy $E(^{24}\mathrm{Mg})=134.5$ MeV from the 88-Inch Cyclotron Facility at Lawrence Berkeley National Laboratory. The 1 mg/cm^2 target consisted of isotopically enriched ^{173}Yb evaporated onto a 7 mg/cm^2 gold backing. The angle between the target and the beam was 27°. The predominant exit channel is ^{192}Pb; these data were also used to study the decay of the yrast superdeformed band in ^{192}Pb [34]. The ^{191}Pb and ^{189}Hg exit channels were the second most predominant; ^{193}Pb, ^{190}Hg, and ^{191}Tl were also identified in this data set.

Gamma rays were detected using the Gammasphere detector array which consisted of 92 large-volume, n-type hyperpure Ge detectors, each surrounded by a BGO Compton-suppression shield and Ta-Cu absorbers in front of the Ge crystals. A total of approximately 2.3×10^9 coincidence events, of three- and higherfold, was collected and stored on magnetic tapes for subsequent off-line analysis.

Gamma rays from standard ^{152}Eu, ^{182}Ta, and ^{56}Co sources were recorded in singles mode for efficiency and energy calibrations. In addition to determining the total efficiency of the array, the efficiency ratio between the set of detectors at 90.0° and the set comprising the 17.3° (forward) and 162.7° (backward) detectors (forward-backward set) has been deduced. This ratio R_{eff} is shown in Fig. 1. Ratio values of $R_{\mathrm{eff}}\approx1.0$ are only observed for $E_\gamma>600$ keV. This is mainly attributed to the higher setting of the low-energy thresholds for the detectors in the forward-backward set and, in particular, those at forward angles, compared to the thresholds for the detectors at 90.0°. To accomodate the efficiency correction necessary in angle-dependent analyses, an empirical function was fit to the ratio

$$R_{\mathrm{eff}}=\exp[(A+Be_1)^{-C}+(D+Fe_2+Ge_2^2)^{-C}]^{-(1/C)}, \quad (1)$$

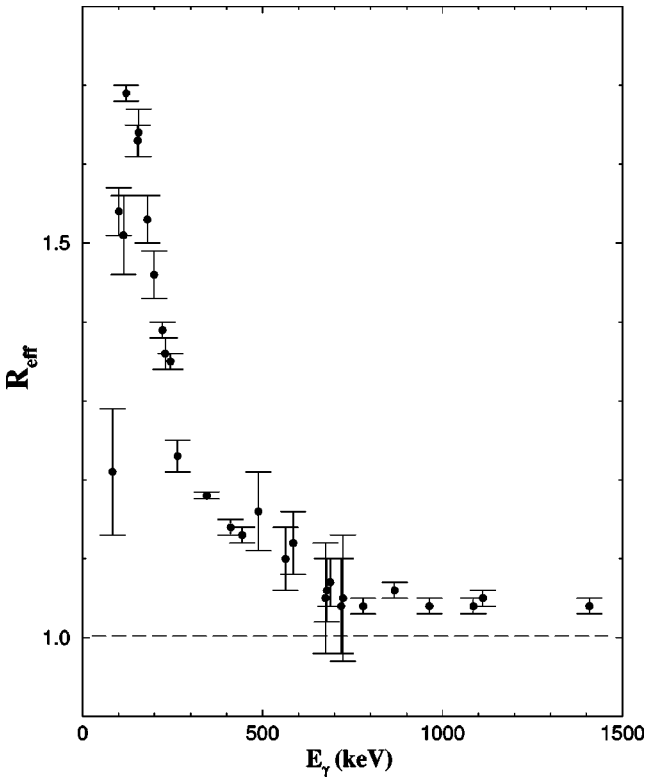

FIG. 1. Ratio $R_{\rm eff}$ between the efficiency of the set of 90.0° detectors and the efficiency of the set comprising the 17.3° (forward) and 162.7° (backward) detectors deduced from spectra of standard ^{152}Eu, ^{182}Ta, and ^{56}Co sources. See text for further discussion.

where $e_1=\log(E/100)$ and $e_2=\log(E/1000)$, for the γ-ray energy, E in keV. The parameters extracted were: $A=0.3973(1)$, $B=0.6474(1)$, $D=0.0364(40)$, $F=-0.0253(1)$, and $G=0.1100(1)$, and $C=30$ was held fixed. The strongly angle-dependent efficiency correction as a function of γ-ray energy noted here is probably unique to the present experiment, because the locations in the array of specific detectors are regularly changed, and often detectors are removed to be reannealed. However, this observation suggests that care is required when angle-dependent analyses are performed.

The recorded data were unpacked into threefold coincidences and stored in a symmetrized, three-dimensional $4096\times4096\times4096$ channel cube, which was used to investigate coincidence relationships between the transitions. The events from the 90.0° and the forward-backward sets of detectors were unpacked into twofold events and stored in a two-dimensional 4096×4096 channel matrix. This matrix was constructed to establish the directional correlations, DCO ratios, of the γ rays, $I(17°+163°;90°)/I(90°;17°+163°)$, where $I(\theta_1;\theta_2)$ is the intensity of a transition recorded by a detector at angle θ_1 when gated on a detector at angle θ_2. The notation $17°+163°$ represents the forward-backward set of detectors, which are actually at 17.3° and 162.7°. The DCO values calculated from this matrix were corrected for the efficiency difference observed between the 90.0° and the forward-backward detector set using the fitted function of Eq. (1). When the gate corresponds to a stretched quadrupole γ ray, a DCO value near 1.0 suggests a stretched quadrupole transition, although a $\Delta J=0$ dipole transition is possible, while a DCO value ≈0.5 suggests a stretched dipole transition, although a $\Delta J=0$ quadrupole is possible. When gating on a stretched dipole transition, a DCO value ≈1.0 indicates a stretched dipole and 2.0 indicates a stretched quadrupole transition, although $\Delta J=0$ transitions of quadrupole and dipole character, respectively, are possible. Since it is unlikely that $M2$ transitions will be observed as prompt γ rays, we assumed that stretched quadrupole transitions are $E2$ in character. Because we have used a heavy-ion-induced reaction, which preferentially populates yrast or near-yrast states, we also assume that $\Delta J<0$ transitions are unlikely, unless a level also has dominant $\Delta J>0$ transitions that depopulate it.

III. EXPERIMENTAL RESULTS

A. Isotopic assignment

The level scheme of ^{191}Pb deduced from the present work is shown in Fig. 2. The four intense transitions, at 818.5, 482.5, 562.1, and 339.0 keV, were previously seen in coincidence with mass 191 with the ^{164,166}Er+164 MeV ^{32}S reaction [33]. In the previous work the possible $A=191$ reaction channels were ^{191}Po ($5n$), ^{191}Bi ($p4n$ and $p6n$), and ^{191}Pb (αn and $\alpha3n$); the only one of these which can be populated in the ^{24}Mg+^{173}Yb reaction is ^{191}Pb. This further supports the assignment of these four transitions and, hence, of the entire level scheme, to ^{191}Pb. There are three additional arguments which support the ^{191}Pb assignment.

(i) Extrapolating the systematics of the $17/2^+$ states in the odd-mass Pb isotopes, displayed in Fig. 3, we expect an energy value in ^{191}Pb for the $17/2^+\rightarrow13/2^+$ transition between 770 and 830 keV. In the total projection of the cube in Fig. 4, the 818.5-keV transition is the only strong transition in this energy range which is in coincidence with Pb x rays.

(ii) The intensity of the 818.5-keV transition is $\approx27\%$ of the intensity of the 853.8-keV transition, which is the strongest transition in ^{192}Pb, as seen in Fig. 4. The $5n$ channel (^{192}Pb) is dominant in the ^{24}Mg+^{173}Yb reaction at 134.5 MeV, for which the ^{191}Pb isotope is the $6n$ channel. This intensity ratio is in accordance with the expected cross-section ratio of the $5n$ and $6n$ reaction channels.

(iii) The levels assigned to ^{191}Pb follow the systematics in Fig. 3 of the corresponding levels in the heavier Pb isotopes. This argument was also used in [33].

B. Level scheme

In the present work 63 transitions connecting 47 levels in ^{191}Pb were identified to establish the level scheme in Fig. 2. All excitation energies of the levels are given relative to the 138-keV excitation energy of the $13/2^+$, 2.18-m isomer [35]. The γ-ray data are summarized in Table I. The placements of the transitions are based on the coincidence relations between these transitions, their relative intensities, and excitation energy sums. Examples of spectra obtained by setting double gates $(E_{\gamma_1},E_{\gamma_2})$ on the γ-γ-γ coincidence cube are displayed in Fig. 5. Tentative spin and parity assignments were made based on DCO ratios and/or the systematics of

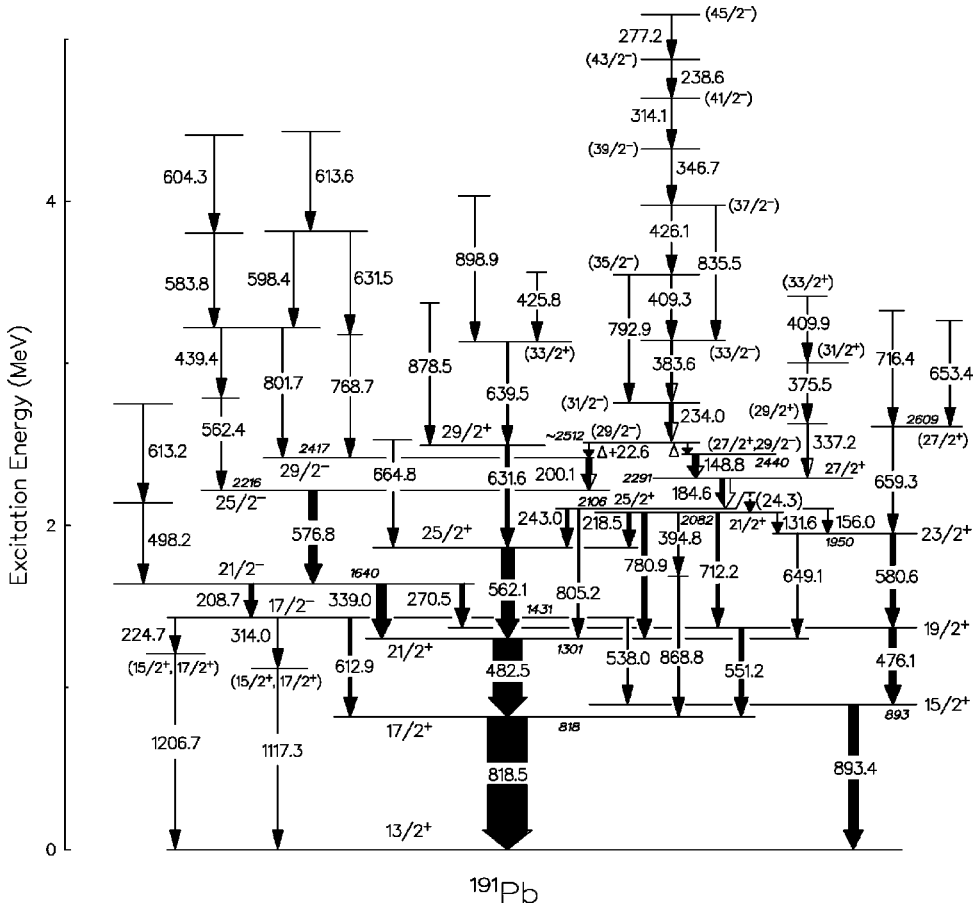

FIG. 2. Level scheme of ^{191}Pb obtained in the present work. The width of the arrows is representative of the intensity of the transitions, while the white part of the arrows is the correction due to expected internal conversion. The γ-ray energies and excitation energies of specified levels are in keV. See text for further discussion.

the heavier odd-mass Pb isotopes [1–10]. In addition, the data suggested three additional low-energy transitions, which will be discussed below.

The most strongly populated levels at low excitation in ^{191}Pb decay by parallel cascades of stretched transitions built on the $13/2^+$ isomer. If we assume that the 818.5-keV transition is $E2$ in character, then the DCO ratios support the 482.5-, 562.1-, and 631.6-keV lines as a stretched $E2$ cascade up to the $29/2^+$ state at 2494 keV. Above this $29/2^+$ level, the regularity of the transition energies ends with a change to a more fragmented structure.

The DCO ratios for the cascade that populates the 893-keV level support the conclusion that the 893.4-keV line is a stretched transition of multipolarity different from the lines that feed the 893-keV level. If we assume that the 893.4-keV line is a stretched $M1$ transition, then the 476.1- and 580.6-keV lines are stretched quadrupole transitions up to the $23/2^+$ state at 1950 keV. Although its intensity is too weak to extract a DCO ratio, we have also assumed that the 659.3-keV transition is of stretched $E2$ character, depopulating the $(27/2^+)$ level at 2609 keV. Above this $(27/2^+)$ state, the level pattern suggests the onset of irregular behavior, similar to that observed for the yrast quasiband.

The 339.0-keV transition was also observed in [33] and placed to depopulate a $21/2^-$ state based on systematics. The present work confirms the placement of this transition. To support the $21/2^-$ assignment, the DCO ratio for the 270-keV line gated on the 893.4-keV stretched dipole transition is consistent with a stretched dipole, which we assume to be $E1$ in character, based on systematics. This $21/2^-$ level at 1640 keV has a $25/2^-$ level above it, with the assignment supported by the DCO ratio for the 576.8-keV line. The $21/2^-$ and $25/2^-$ levels follow the systematics of these states in the odd-mass Pb istotopes, as displayed in Fig. 3. Unlike the $21/2^-$ levels in the heavier isotopes, this state in ^{191}Pb does not appear to be isomeric, because of the relatively large energy ($E_\gamma = 339.0$ keV) available for the $21/2^- \rightarrow 21/2^+$ transition, compared, for example, to the 184.3-keV energy for this transition in ^{193}Pb [2].

The sequence of eight transitions, 234.0, 383.6, 409.3, 426.1, 346.7, 314.1, 238.6, and 277.2 keV, is similar to sequences which have been assigned to $M1$ bands in the heavier Pb isotopes [1–10]. Henceforth, we will refer to this sequence as dipole band 1. A spectrum associated with gates on transitions in the band is displayed in Fig. 5(a). Because of low statistics, a DCO ratio consistent with stretched dipole character could only be determined for the lowest transition at 234.0 keV. We have assumed $M1$ character for this line, and based on systematics, have tentatively assigned $M1$ to the other transitions in this cascade. In the middle of the band, above the 426.1-keV transition, a backbending is observed. Two weak, crossover transitions, at 792.9 and 835.5 keV, have been placed. These transitions are presumably $E2$ in character, although no DCO ratio determination was pos-

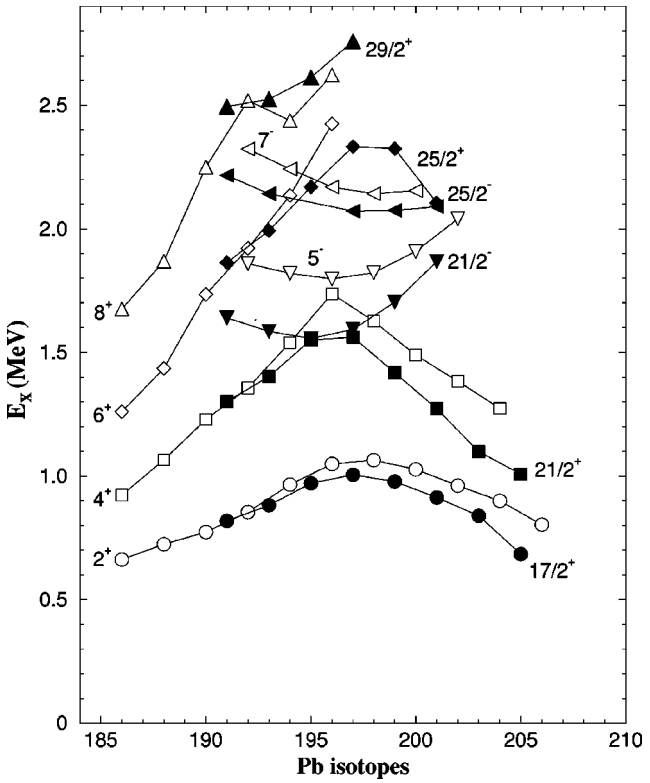

FIG. 3. Systematics of the excitation energies of the 17/2, 21/2, 25/2, and 29/2 positive-parity states and the 21/2 and 25/2 negative-parity states in the odd-mass Pb isotopes (solid symbols) together with the 2, 4, 6, and 8 positive-parity states and the 5 and 7 negative-parity states in the even-mass Pb isotopes (open symbols). Excitation energies of the states are taken from [35] and the present work.

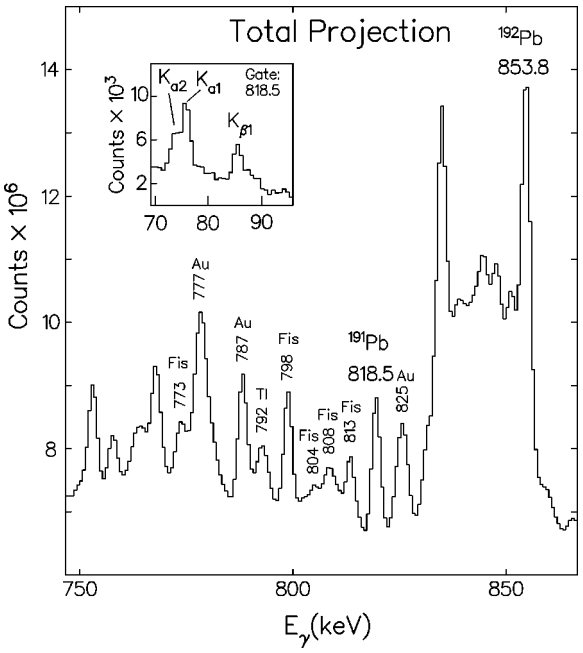

FIG. 4. Part of the total projection spectrum of the γ-γ-γ coincidences cube. The energies of the transitions are given in keV. Transitions from fission products are labeled as ''Fis'' while transitions from the gold backing are labeled as ''Au.'' The inset shows the Pb x rays from the gate on the 818.5-keV transition.

sible. The ordering of the transitions is based on intensity and coincidence arguments associated with the crossover transitions.

The intensity of dipole band 1 in ^{191}Pb is $\sim$10% of the intensity of the channel, determined from the intensity of the 234.0-keV transition corrected for conversion. This strong population in the reaction channel is similar to what is observed for the dominant dipole bands in the heavier Pb isotopes [1–10].

It is difficult to assign excitation energy and spin-parity values for this proposed dipole band 1, without invoking the systematical behavior of the strongest $M1$ bands observed in the heavier Pb isotopes. The deexcitation of the proposed $M1$ band 1 in ^{191}Pb is fragmented along two paths, which involve low-energy transitions.

The first path itself is fragmented and carries $\sim$60% of the band intensity towards the lower-lying positive-parity levels. This path involves the 148.8- and 184.6-keV transitions, both of stretched dipole character, or $\Delta J=0$ quadrupoles, based on their DCO ratios. We have ordered these transitions based on coincidence relations with the cascade built on the 337.2-keV line. With the proposed ordering, intensity arguments require the 184.6-keV line to have $M1$ multipolarity.

The fragmentation of the first deexcitation path for dipole band 1 proceeds by feeding two close-lying excited states at 2082 and 2106 keV, which are separated by only 24.3 keV. Because the transitions above the 2106-keV level and below the 2082-keV level are in coincidence, a 24.3-keV transition connecting these levels should be present. However, because of intense conversion, low-energy discriminator levels, and attenuation by the Ta-Cu absorbers, such a transition is impossible to observe in our experiment. The spin and parity of these levels have been established, $25/2^+$ for the 2106-keV level and $21/2^+$ for the 2082-keV level, based on DCO ratios of transitions feeding states in the dominant stretched $E2$ cascades. A similar case of two close-lying levels (6 keV apart) has been observed in the deexcitation of the strongest negative-parity dipole band in ^{195}Pb [5].

The second deexcitation path of dipole band 1 bypasses the $(2082+2106)$-keV pair of levels and carries the remaining $\sim$40% of the intensity to the negative-parity states at lower excitation. This fraction was determined by the ratio of intensities (corrected for internal conversion) of the 148.8- and 200.1-keV transitions.

The two paths by which the proposed dipole band 1 deexcites to the low-lying states do not converge on the same initial level. Also, the systematics of the excitation energies of the strong dipole bands in the heavier isotopes suggest that additional low-energy transitions are probably involved in the decay of $M1$ band 1 in ^{191}Pb. First, we would like to propose that the spin parity of the head of the $M1$ band in ^{191}Pb, the level fed by the 234.0-keV transition, is $29/2^-$, as is the case for the strongest $M1$ bands in the heavier isotopes. We also propose that both deexcitation paths involve low-energy ($E_\gamma<100$ keV) transitions. Such transitions would not be observed in our spectra because they are highly converted, attenuated by the Ta-Cu absorbers, and obscured by the Pb x rays. For the first path, we tentatively suggest the existence of a Δ-keV transition between the $M1$ bandhead

TABLE I. Energies, intensities, DCO ratios, excitations, and assignment for all transitions in ^{191}Pb. Values in parentheses are not firmly established. DCO values marked with an asterisk were obtained by gating on a $\Delta I = 1$ dipole transition.

Energy[a] (keV)	Intensity[b] (‰)	DCO	Excitation[c] E_i (keV)	E_f (keV)	Assignment I_i^π	↦	I_f^π
131.6	<5		2081.9	1950.2	$\frac{21}{2}^+$	↦	$\frac{23}{2}^+$
148.8	140(10)	0.54(5)	2439.6	2290.8	$(\frac{27}{2}^+, \frac{29}{2}^-)$	↦	$\frac{27}{2}^+$
156.0	<5		2106.2	1950.2	$\frac{25}{2}^+$	↦	$\frac{23}{2}^+$
184.6	105(10)	0.48(4)	2290.8	2106.2	$\frac{27}{2}^+$	↦	$\frac{25}{2}^+$
200.1	100(10)	1.05(5)	2416.9	2216.8	$\frac{29}{2}^-$	↦	$\frac{25}{2}^-$
208.7	100(10)		1640.0	1431.4	$\frac{21}{2}^-$	↦	$\frac{17}{2}^-$
218.5	80(8)		2081.9	1863.1	$\frac{21}{2}^+$	↦	$\frac{25}{2}^+$
224.7	8(2)		1431.4	1206.7	$\frac{17}{2}^-$	↦	$(\frac{15}{2}^+, \frac{17}{2}^+)$
234.0	56(8)	0.47(8)	2746.1	2512.1	$\frac{31}{2}^-$	↦	$\frac{29}{2}^-$
238.6	6(2)		4864.5	4625.9	$(\frac{43}{2}^-)$	↦	$(\frac{41}{2}^-)$
243.0	75(7)	1.07(10)	2106.2	1863.1	$\frac{25}{2}^+$	↦	$\frac{25}{2}^+$
270.5	115(10)	0.79(15)	1640.0	1369.6	$\frac{21}{2}^-$	↦	$\frac{18}{2}^+$
277.2	<5		5141.7	4864.5	$(\frac{45}{2}^-)$	↦	$(\frac{43}{2}^-)$
314.0	25(5)		1431.4	1117.3	$\frac{17}{2}^-$	↦	$(\frac{15}{2}^+, \frac{17}{2}^+)$
314.1	7(2)		4625.9	4311.8	$(\frac{41}{2}^-)$	↦	$(\frac{39}{2}^-)$
337.2	33(5)		2628.0	2290.8		↦	$\frac{27}{2}^+$
339.0	235(20)	1.01(7)	1640.0	1301.0	$\frac{21}{2}^-$	↦	$\frac{21}{2}^+$
346.7	8(2)		4311.8	3965.1	$(\frac{39}{2}^-)$	↦	$(\frac{37}{2}^-)$
375.5	17(5)		3003.5	2628.0			
383.6	44(8)		3129.7	2746.1	$(\frac{33}{2}^-)$	↦	$\frac{31}{2}^-$
394.8	26(5)		2081.9	1687.3	$\frac{21}{2}^+$	↦	
409.3	27(6)		3539.0	3129.7	$(\frac{35}{2}^-)$	↦	$(\frac{33}{2}^-)$
409.9	8(2)		3413.4	3003.5			
425.8	<5		3560.0	3134.2		↦	$(\frac{33}{2}^+)$
426.1	19(3)		3965.1	3539.0	$(\frac{37}{2}^-)$	↦	$(\frac{35}{2}^-)$
439.4	8(2)		3218.6	2779.2			
476.1	170(10)	1.75(10)	1369.6	893.4	$\frac{19}{2}^+$	↦	$\frac{15}{2}^+$
482.5	740(30)	0.98(5)	1301.0	818.5	$\frac{21}{2}^+$	↦	$\frac{17}{2}^+$
498.2	10(3)		2138.2	1640.0		↦	$\frac{21}{2}^-$
538.0	26(5)	1.05(30)	1431.4	893.4	$\frac{17}{2}^-$	↦	$\frac{15}{2}^+$
551.2	100(10)		1369.6	818.5	$\frac{19}{2}^+$	↦	$\frac{17}{2}^+$
562.1	330(30)	1.02(6)	1863.1	1301.0	$\frac{25}{2}^+$	↦	$\frac{21}{2}^+$
562.4	17(4)		2779.2	2216.8		↦	$\frac{25}{2}^-$
576.8	200(20)	1.05(6)	2216.8	1640.0	$\frac{25}{2}^-$	↦	$\frac{21}{2}^-$
580.6	115(10)	2.3(4)	1950.2	1369.6	$\frac{23}{2}^+$	↦	$\frac{19}{2}^+$
583.8	8(2)		3802.4	3218.6			
598.4	7(2)		3817.0	3218.6			
604.3	<5		4406.7	3802.4			
612.9	50(10)	1.01(9)	1431.4	818.5	$\frac{17}{2}^-$	↦	$\frac{17}{2}^+$
613.2	<5		2751.4	2138.2			
613.6	<5		4430.6	3817.0			
631.5	<5		3817.0	3185.6			
631.6	105(10)	0.99(10)	2494.7	1863.1	$\frac{29}{2}^+$	↦	$\frac{25}{2}^+$
639.5	30(5)		3134.2	2494.7	$(\frac{33}{2}^+)$	↦	$\frac{29}{2}^+$
649.1	24(5)		1950.2	1301.0	$\frac{23}{2}^+$	↦	$\frac{21}{2}^+$
653.4	11(3)		3262.9	2609.5		↦	$(\frac{27}{2}^+)$
659.3	21(5)		2609.5	1950.2	$(\frac{27}{2}^+)$	↦	$\frac{23}{2}^+$
664.8	26(5)		2527.9	1863.1		↦	$\frac{25}{2}^+$
712.2	62(7)		2081.9	1369.6	$\frac{21}{2}^+$	↦	$\frac{19}{2}^+$

TABLE I. (*Continued*).

Energy[a] (keV)	Intensity[b] (‰)	DCO	Excitation[c] E_i (keV)	E_f (keV)	Assignment I_i^π	$\mapsto$	I_f^π
716.4	9(2)		3325.9	2609.5		$\mapsto$	$(\frac{27}{2}^+)$
768.7	7(2)		3185.6	2416.9		$\mapsto$	$\frac{29}{2}^-$
780.9	120(10)	1.05(8)	2081.9	1301.0	$\frac{21}{2}^+$	$\mapsto$	$\frac{21}{2}^+$
792.9	6(2)		3539.0	2746.1	$(\frac{35}{2}^-)$	$\mapsto$	$\frac{31}{2}^-$
801.7	12(3)		3218.6	2416.9		$\mapsto$	$\frac{29}{2}^-$
805.2	55(5)		2106.2	1301.0	$\frac{25}{2}^+$	$\mapsto$	$\frac{21}{2}^+$
818.5	$\equiv$1000	1.05(7)	818.5	0.0	$\frac{17}{2}^+$	$\mapsto$	$\frac{13}{2}^+$
835.5	5(2)		3965.1	3129.7	$(\frac{37}{2}^-)$	$\mapsto$	$(\frac{33}{2}^-)$
868.8	44(8)		1687.3	818.5		$\mapsto$	$\frac{17}{2}^+$
878.5	8(2)		3373.2	2494.7		$\mapsto$	$\frac{29}{2}^+$
893.4	240(20)	0.42(7)	893.4	0.0	$\frac{15}{2}^+$	$\mapsto$	$\frac{13}{2}^+$
898.9	<5		4033.1	3134.2		$\mapsto$	$(\frac{33}{2}^+)$
1117.3	13(3)		1117.3	0.0	$(\frac{15}{2}^+, \frac{17}{2}^+)$	$\mapsto$	$\frac{13}{2}^+$
1206.7	6(2)		1206.7	0.0	$(\frac{15}{2}^+, \frac{17}{2}^+)$	$\mapsto$	$\frac{13}{2}^+$

[a]The uncertainties on the γ-ray energies vary from 0.2 to 0.4 keV for the strong transitions and from 0.8 to 1.0 keV for the weakest ones.
[b]Intensities relative to the intensity of the 818.5-keV transition derived from coincidence gates.
[c]The uncertainty on the excitation varies from 0.2 to 0.8 keV. The uncertainty in the excitations for the levels of the dipole band 1 is 5 keV (see text).

and 2440-keV level. A possible value for Δ based on systematics is discussed in Sec. IV B.

For the second deexcitation path, we propose a direct $(\Delta+23.6)$-keV transition and/or a two-step path, via the 2440-keV level, which connects the dipole bandhead and the $29/2^-$ level at 2417 keV. Again, it is unlikely we could observe such low-energy transitions with the present experimental conditions.

The dipole bandhead is probably an isomer because of the low-energy transitions which depopulate this state. This is also the case for the strongest negative-parity dipole band in the neighboring ^{193}Pb isotope [2,3,29], where the lifetime of the $29/2^-$ isomer is 13.6(10) ns [29].

Above the $27/2^+$, 2291-keV level a sequence of three weak transitions has been observed (337.2, 375.5, and 409.9 keV). This sequence could be a second dipole band in ^{191}Pb, but the statistics are not sufficient to establish a DCO ratio for these transitions. However, in most of the heavier Pb isotopes more than one dipole band has been observed, a fact that leads us to expect the presence of more than one dipole band in ^{191}Pb. Moreover, this sequence in ^{191}Pb is almost identical to dipole band 3 of ^{193}Pb [2]: Both sequences are built on the $27/2^+$ state at about the same excitation energy and the transitions have similar energies. As expected from systematics, the excitation energies in ^{191}Pb are slightly lower than in ^{193}Pb. The crossover transitions which would be associated with this second dipole band in ^{191}Pb are not observed, because they would have very low intensity. These similarities strongly suggest that this sequence of three transitions above the $27/2^+$ state at 2291 keV determines the first levels of a dipole band 2, of positive parity, in ^{191}Pb.

The remainder of the level scheme in Fig. 2 forms the spherical level scheme of irregularly spaced levels of positive or negative parity, similar to spherical level schemes observed in the heavier odd-mass Pb isotopes [1–10]. The levels determined by the 1117.3- and 1206.7-keV transitions are worth highlighting. Given the DCO ratios for the 538.0- and 612.9-keV transitions to the $15/2^+$ and $17/2^+$ states, respectively, and the placement of the 208.7-keV line depopulating the $21/2^-$ level, the only allowed J^π for the 1431-keV level is $17/2^-$. Given that the 1117.3- and 1206.7-keV lines feed the $13/2^+$ isomer and are fed by the $17/2^-$ state, we propose $(15/2^+,17/2^+)$ assignments for the 1117- and 1206-keV levels. A non-$M1$ character for the 224-keV line is preferred, to preserve the intensity balance associated with the 1206-keV level. Similar states have been established in ^{197}Pb and ^{199}Pb [7–10].

IV. DISCUSSION

A. Spherical states

The pattern of the lower part of the ^{191}Pb level scheme is similar to the corresponding parts of the level schemes in the heavier Pb isotopes and suggests a single-particle, weakly collective, nuclear motion. In Fig. 6 we summarize the yrast states in ^{190,192,194}Pb and compare them to excitations in ^{191,193}Pb.

The first excited positive-parity levels in ^{191}Pb at 818 and 893 keV arise from the coupling of a hole in the neutron $i_{13/2}$ orbital to the first positive-parity, 2^+ state of the even ^{192}Pb core at 854 keV [1]. The $[i_{13/2}\otimes 2^+]$ configuration gives rise to a multiplet of states, of which we expect the $17/2^+$ and $15/2^+$ members to be lowest in energy. This weak-coupling picture reproduces the trends in energies of the $17/2^+$ state at 818 keV compared to the 893- and 774-keV energies of the 2^+ states in the neighboring ^{192}Pb and ^{190}Pb cores, respectively. As summarized in Fig. 6, this weak-coupling picture extends to the $21/2^+$,$19/2^+$ multiplet, from coupling to the 4^+ state at 1356 keV in ^{192}Pb; the $25/2^+$,$23/2^+$ multiplet

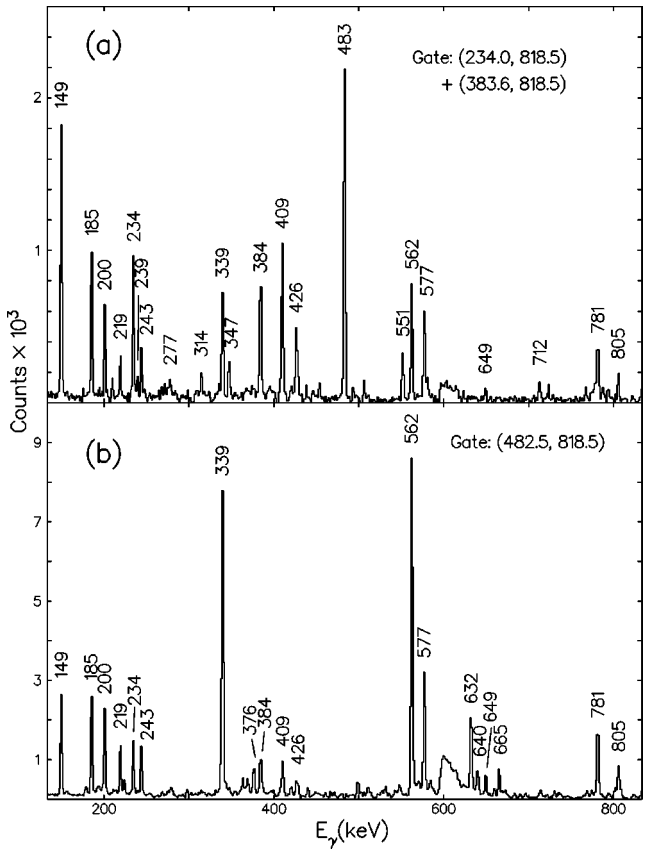

FIG. 5. Selected spectra obtained from double gates on the γ-γ-γ coincidence cube from the ^{24}Mg+^{173}Yb reaction at 134.5 MeV: (a) background-subtracted spectrum from the (482.5, 818.5)-keV gate, (b) sum of background-subtracted spectra from the (234.0, 818.5)-keV and (383.6, 818.5)-keV gates.

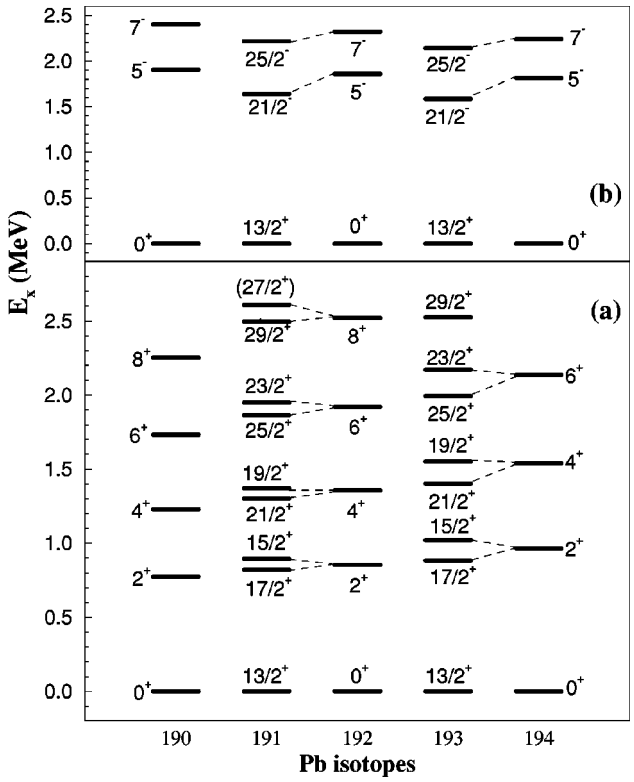

FIG. 6. Systematics of the yrast positive- and negative-parity states in ^{190,192,194}Pb compared to candidates for weakly coupled states in ^{191,193}Pb. Data taken from [35] and the present work.

from coupling to the 6^+ state at 1921 keV in ^{192}Pb; and the $29/2^+$, $(27/2^+)$ multiplet from coupling to the 8^+ state at 2520 keV in ^{192}Pb. The nonyrast $(15/2^+,17/2^+)$ states at 1117 and 1206 keV could be the weakly coupled states associated with the 2_2^+ state at 1237.9 keV in ^{192}Pb. In addition to these positive-parity states, the $21/2^-$ and $25/2^-$ negative-parity states at 1640 and 2216 keV, respectively, are proposed as arising from the coupling to the 5^- and 7^- states at 1860 and 2303 keV in ^{192}Pb, respectively. That the state with maximum angular momentum, which arises from a weak coupling of the neutron $i_{13/2}$ orbital to the 5^- state of the core, is not yrast in ^{191}Pb, reflects the importance of the neutron $i_{13/2}$ unique-parity orbital in the negative-parity 5^- configuration in the core.

B. Dipole band

The dipole band 1 built on the 234.0-keV transition in Fig. 2 dominates the upper part of the level scheme of ^{191}Pb with intensity $>10\%$. This band is regular up to spin $37/2^-$, then undergoes a backbending, and becomes regular again above the $41/2^-$ level. In Fig. 7 the alignment of dipole band 1 of ^{191}Pb is shown as a function of the rotational frequency. From this figure it can be seen that the backbending starts at about $\hbar\omega\sim 0.34$ MeV and suggests a crossing frequency of about $\hbar\omega_c\sim 0.28$ MeV.

The similarities with the strongest bands reported in the heavier odd-mass Pb isotopes [2,3,5,7,8] are striking. As in the heavier odd-A Pb isotopes displayed in Fig. 8, the proposed $M1$ band 1 in ^{191}Pb is a strongly populated cascade of transitions with energies similar to those in the heavier isotopes and following the trend of a backbend at frequency $\hbar\omega_c\approx 0.3$ MeV.

In order to highlight this similarity in the sequence of transitions, the spins of the levels above the $29/2^-$ level of these $M1$ bands are shown in Fig. 8(a) as a function of rotational frequency. It can be seen that, except in the case of ^{193}Pb, all of the curves are almost identical. The band in question in ^{193}Pb has been reported as dipole band 1a by Baldsiefen *et al.* in [2] and as dipole band 1 by Ducroux *et al.* in [3]. This exception in the case of ^{193}Pb led us to question the spin assignment of the dipole band levels in ^{193}Pb, because we have no reason to expect such an exception. Furthermore, if one shifts the spin assignment in these levels by $-1\hbar$, the curve shown in Fig. 8(b) for the dipole band of ^{193}Pb is obtained. It is clear from Fig. 8(b) that this shift results in a sequence of level spins in ^{193}Pb very similar to all the neighboring odd-mass Pb isotopes. A second argument supporting this shifting is illustrated in Fig. 9, where the evolution in the odd-mass Pb isotopes of the excitation energies of the $29/2^-$ and $31/2^-$ levels of the dipole bands, relative to the excitation energy of the $13/2^+$ isomer, is shown. With the existing assignment, a discontinuity in this evolution appears in ^{193}Pb (dashed lines in Fig. 9), while by shifting the spin assignment by $-1\hbar$, this discontinuity disappears and a gradual downward trend in the excitation energies of these states is established (solid lines in Fig. 9). It

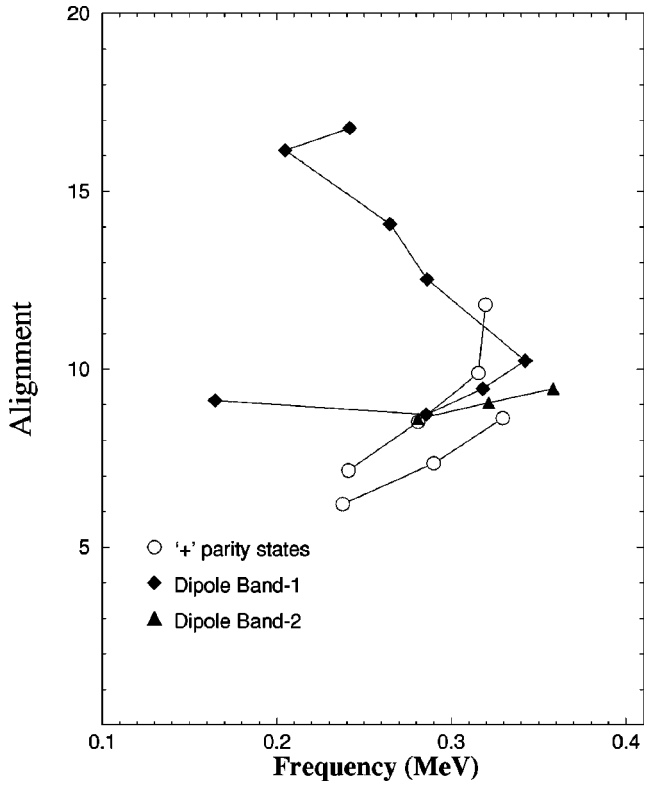

FIG. 7. Alignment in units of $\hbar$ of the quadrupole and dipole bands of ^{191}Pb as a function of rotational frequency $\hbar\omega$, in MeV. An alignment of $(10\omega+30\omega^2)\hbar$ for the core has been subtracted based on the Harris parameters for ^{191}Hg [36]. $K=11$ has been used for dipole band 1 and $K=8$ for dipole band 2.

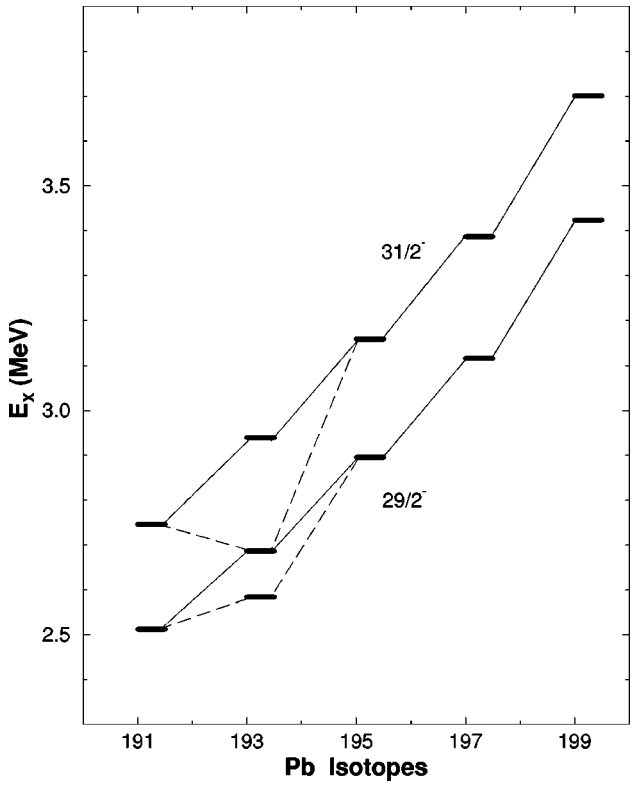

FIG. 9. Systematics of the excitation energies of the $29/2^-$ and $31/2^-$ levels of the strongest negative-parity dipole bands in odd-mass $^{191-199}$Pb isotopes ([3,4,6,8,9], present work) (solid lines) relative to the excitation energy of the $13/2^+$ isomer. The published results [2,3] for ^{193}Pb are indicated by dashed lines. By shifting the spins of the levels of the strongest negative-parity dipole band in ^{193}Pb by $-1\hbar$ the solid-line systematics is obtained.

should be noted that plotting the excitation energies with respect to the excitation energy of the ground state leads to almost the same picture without affecting the discontinuity in ^{193}Pb. A third argument comes from the extrapolation of the systematics of the transitions depopulating the $29/2^-$ member of the strong dipole bands in ^{195,197,199}Pb. This extrapolation results in a 108-keV transition in ^{193}Pb, almost equal to the observed 102-keV line, which has been reported as the $31/2^-\rightarrow 29/2^-$ transition [2,3,29]. It is on the basis of these three arguments that we suggest here that the spin assignment in the strongest negative-parity dipole band of ^{193}Pb should be reconsidered. It is more likely that the spin of the $31/2^-$ level at 2686 keV [2,3,29] is $29/2^-$. Likewise, the spin of all the dipole band levels, as well as all the reported levels above this level, should be shifted by $-1\hbar$.

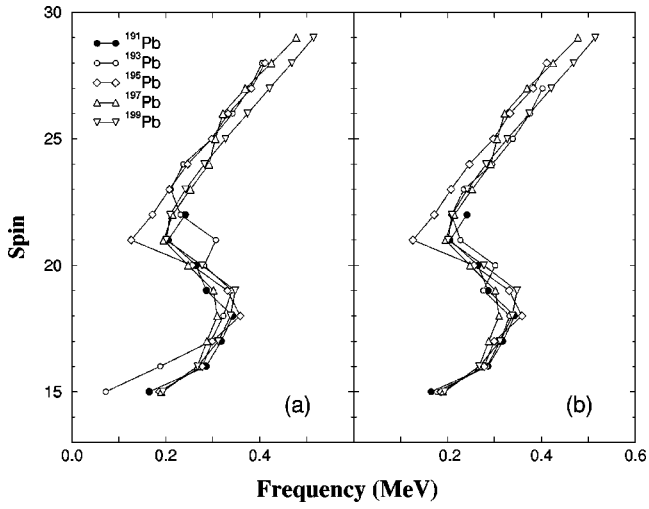

FIG. 8. (a) Spin in units of $\hbar$ as a function of rotational frequency $\hbar\omega$, in MeV, for the strongest negative-parity dipole bands observed in odd-mass $^{191-199}$Pb isotopes ([3,4,6,8,9], present work). (b) Same as in (a) except that the spins of the levels of the strongest negative-parity dipole band in ^{193}Pb [2,3] have been shifted by $-1\hbar$ (see text).

Based on the systematics for dipole bands displayed in Figs. 8 and 9, we propose a value of $\approx$72 keV for the low-energy transition Δ at the bottom of dipole band 1 in ^{191}Pb, as well as a $29/2^-$ spin assignment for the bandhead fed by the 234.0-keV transition. For the corresponding dipole bands observed in ^{195}Pb [5], ^{197}Pb [7], and ^{199}Pb [8] the $29/2^-$ to $27/2^-$ transitions are reported to be 129.7, 152.6, and 173.9 keV, respectively. In the case of ^{193}Pb the corresponding transition depopulating the $29/2^-$ state is 102 keV, as discussed above. A 72-keV value for the transition depopulating the $29/2^-$ state in ^{191}Pb is expected after extrapolating the decrease of the energy of these transitions in the heavier Pb isotopes. Almost the same value (69.8 keV) is obtained if one extrapolates the excitation energies of the corresponding levels, to determine the transition energy. Hence, a 72 $\pm$5 keV energy for the $29/2^-\rightarrow 27/2^-$ transition in ^{191}Pb has been adopted, which determines the uncertainty of $\pm$5 keV

in the excitation energies of the levels of dipole band 1 reported in Table I.

Apart from the similarities established above, there is a difference between dipole band 1 in ^{191}Pb and the corresponding dipole bands in the heavier odd-mass Pb isotopes. In ^{191}Pb dipole band 1 deexcites to negative-parity spherical states, as well as to positive-parity states, with comparable intensities in the two branches. In contrast, in the heavier odd-mass Pb isotopes the corresponding dipole bands deexcite only to lower-lying positive-parity states, although negative-parity states are available.

The ''shears'' effect [8,30] has been suggested to account for the gain of spin within the dipole bands in the Pb region. According to this picture, at the bandhead the spins of the proton particles and neutron holes are perpendicular to each other, resulting in a total spin pointing somewhere in between these vectors. Within the band, the total spin increases as the spin of both the proton particles and the neutron holes align gradually onto the direction of the total spin, like the closing of the blades in a pair of shears, hence the name shears effect. The tilted axis cranking model [30] (TAC) has been successfully used to describe quantitatively this effect. In the Pb isotopes, two proton particles below the $Z=82$ shell gap (from the $s_{1/2}$ orbital) are excited into orbitals above the gap ($h_{9/2}$ and/or $i_{13/2}$), align with the symmetry axis (high-K orbitals), and drive the core to oblate deformation. On the other hand, the neutron orbitals close to the Fermi level are the $i_{13/2}$ orbitals, which, at oblate deformation, prefer to align with the collective rotation axis (low-K orbitals). Thus, the picture of the total spin pointing somewhere in between the rotation and symmetry axis emerges.

It is expected [30] that the $M1$ bands will become less regular, and eventually disappear, as the Pb isotopes become more collective and the middle of the neutron shell is approached. The increase in level density as the nucleus becomes less spherical would increase the mixing between $M1$ configurations and other excitations at moderate energy and spin. However, the excitation energies of the $M1$ bands, displayed in Fig. 9, decrease as the neutron number decreases. This decrease in excitation energy could compensate for the increased level density expected in more collective nuclei with additional valence neutrons and result in an $M1$ band in ^{191}Pb which exhibits the same regular behavior as analogous bands in heavier isotopes.

The proposed configurations for the dipole bands in ^{191}Pb are summarized in Table II. For all of the strongest negative-parity bands in the heavier odd-mass Pb isotopes the $\pi[s_{1/2}^{-2}h_{9/2}i_{13/2}]_{11}\otimes\nu[i_{13/2}^{-1}]_{13/2}$ configuration has been used to interpret the bandhead [2,3,5,7,8,10]. This configuration also reproduces the empirical g factor [29] for the isomer at the bottom of this dipole band in ^{193}Pb. Using the TAC model abbreviations the above configuration is written as $A11$. In this model the neutron configurations follow the standard cranking shell model convention, while the proton configurations are only labeled by the total proton spin. Based on the above-established striking similarities between these bands and the dipole band observed in ^{191}Pb in this work, we suggest that the same configurations should be used to interpret this band. Above the backbending, in all of the heavier odd-mass Pb dipole bands, the additional alignment of two more neutron holes from the $i_{13/2}$ orbital along the rotational axis has been invoked. This alignment adds 10 units to the total angular momentum on the rotational axis. Hence, the resulting configuration above the backbend is now $\pi[s_{1/2}^{-2}h_{9/2}i_{13/2}]_{11}\otimes\nu[i_{13/2}^{-3}]_{33/2}$ or $ABC11$ in TAC notation. In the case of ^{191}Pb, displayed in Fig. 7, the $\approx 9\hbar$ gain in alignment of dipole band 1 above the backbending suggests that the additional alignment of the two-neutron holes is also the case here.

TABLE II. Configurations proposed for the interpretation of the dipole bands observed in ^{191}Pb.

Protons	Neutrons	TAC notation
	Dipole band 1	
$[s_{1/2}^{-2}h_{9/2}i_{13/2}]11^-$	$[i_{13/2}^{-1}]13/2^+$	$A11$
	and	
$[s_{1/2}^{-2}h_{9/2}i_{13/2}]11^-$	$[i_{13/2}^{-3}]33/2^+$	$ABC11$
	Dipole band 2	
$[s_{1/2}^{-2}h_{9/2}^{2}]8^+$	$[i_{13/2}^{-1}]13/2^+$	$A8$
	or	
$[s_{1/2}^{-1}i_{13/2}]7^+$	$[i_{13/2}^{-1}]13/2^+$	$A7$

Assuming $M1$ and $E2$ multipolarity for the in-band and crossover transitions, respectively, the $B(M1)/B(E2)$ ratios in ^{191}Pb for the $35/2^-$ and $37/2^-$ levels are 23 ± 5 and 20 ± 5 $\mu_N^2/(e\mathrm{b})^2$, respectively. These values are comparable to the $B(M1)/B(E2)$ values reported for the dipole bands in ^{191}Pb [2,3] and ^{195}Pb [5] and tend to be smaller than the values reported in the heavier odd-mass Pb isotopes [7–10]. In [2] it is suggested that this fact may be evidence for the tendency of the neutron system towards prolate deformation, which, in turn, is supported by recent shell model studies of the shears bands [37]. The $B(M1)/B(E2)$ values reported in ^{191}Pb may be further evidence for this effect.

The candidate for a second dipole band in ^{191}Pb exhibits similarities to a positive-parity dipole band in ^{193}Pb [2,3]. Two possible configurations have been proposed for this band in ^{193}Pb: the 2p-2h $\pi[s_{1/2}^{-2}h_{9/2}^{2}]_8\otimes\nu[i_{13/2}^{-1}]_{13/2}$ configuration ($A8$ in TAC notation) or the 1p-1h $\pi[s_{1/2}^{-1}i_{13/2}]_7\otimes\nu[i_{13/2}^{-1}]_{13/2}$ configuration ($A7$ in TAC notation). Both configurations are possible because they reproduce the lower spin and excitation energy of this band with respect to the other dipole bands identified in ^{193}Pb and heavier isotopes. Based on the similarities between this band in ^{193}Pb and the candidate dipole band 2 in ^{191}Pb, the same configurations could be adopted for both.

V. CONCLUSIONS

Excitations in ^{191}Pb have been studied using in-beam γ-ray spectroscopy with the Gammasphere array following the ^{173}Yb(^{24}Mg,6n) at 134.5 MeV. The level scheme of ^{191}Pb above the $13/2^+$ isomer has been enriched and extended up to $\sim$5.1 MeV excitation energy and spin $(45/2^-)$.

A spherical lower part of the level scheme has been established. We observe two cascades of $E2$ transitions which define two members each of the multiplets which arise from coupling the $i_{13/2}$ neutron to the 2^+, 4^+, 6^+, 8^+, and 2_2^+ states of the ^{192}Pb core. We also observe weak coupling of

the $i_{13/2}$ neutron to the 5^- and 7^- states in the core.

At higher excitations a strong negative-parity $M1$ band, dipole band 1, has been found to dominate the level scheme. Comparison of this band with the strongest negative-parity dipole bands in the heavier odd-mass Pb isotopes reveals striking similarities between them. This comparison led to a suggestion that the spin assignment be reconsidered for the levels of the strongest negative-parity dipole band in ^{193}Pb. Based on the similarity with positive-parity $M1$ cascades in heavier isotopes, we have also identified a sequence of three transitions as a candidate for a second dipole band in ^{191}Pb.

The dipole band 1 in ^{191}Pb has a regular sequence of transitions, including a backbend at $\hbar\omega_c \sim 0.28$ MeV, which is similar to observations in the heavier Pb isotopes. High-K proton 2p-2h excitations coupled to high-j neutron holes were invoked for the interpretation of the dipole bands in ^{191}Pb. They involve proton excitations from the $s_{1/2}$ orbital, below the $Z=82$ proton shell, to the $h_{9/2}$ and/or $i_{13/2}$ orbitals above the shell gap. Classifications as magnetic rotations within the TAC formalism [30,38] have been suggested for both dipole bands. The similarities between dipole band 1 in ^{191}Pb and the $M1$ bands observed in the heavier isotopes not only supports the same multiparticle configuration for the ^{191}Pb band, but also demonstrates the persistence of the proposed magnetic rotation [38] in an $N=109$ isotope.

ACKNOWLEDGMENTS

We would like to thank the staff at the 88-Inch Cyclotron for excellent operation of the accelerator and Professor S. Frauendorf for stimulating discussions. This work has been supported in part by the National Science Foundation (Rutgers) and the U.S. Department of Energy, under Contract Nos. W-7405-ENG-48 (LLNL) and AC03-76SF00098 (LBNL).

[1] J. M. Lagrange *et al.*, Nucl. Phys. **A530**, 437 (1991).
[2] G. Baldsiefen *et al.*, Phys. Rev. C **54**, 1106 (1996).
[3] L. Ducroux *et al.*, Z. Phys. A **356**, 241 (1996).
[4] M. Pauprat *et al.*, Phys. Scr. **34**, 378 (1986).
[5] M. Kaci *et al.*, Z. Phys. A **354**, 267 (1996).
[6] M. Pauprat *et al.*, Nucl. Phys. **A443**, 172 (1985).
[7] G. Baldsiefen *et al.*, Nucl. Phys. **A587**, 562 (1995).
[8] G. Baldsiefen *et al.*, Nucl. Phys. **A574**, 521 (1994).
[9] M. Neffgen *et al.*, Nucl. Phys. **A595**, 499 (1995).
[10] G. Baldsiefen *et al.*, Nucl. Phys. **A592**, 365 (1995).
[11] R. M. Clark *et al.*, Phys. Lett. B **275**, 247 (1992).
[12] G. Baldsiefen *et al.*, Phys. Lett. B **275**, 252 (1992).
[13] R. M. Clark *et al.*, Z. Phys. A **342**, 371 (1992).
[14] G. Baldsiefen *et al.*, Z. Phys. A **343**, 245 (1992).
[15] A. Kuhnert *et al.*, Nucl. Phys. **A553**, 567c (1993).
[16] N. Roy *et al.*, Phys. Rev. C **47**, R930 (1993).
[17] J. R. Hughes *et al.*, Phys. Rev. C **47**, R1337 (1993).
[18] B. Cederwall *et al.*, Phys. Rev. C **47**, R2443 (1993).
[19] G. Baldsiefen *et al.*, Phys. Lett. B **298**, 54 (1993).
[20] R. M. Clark *et al.*, J. Phys. G **19**, L57 (1993).
[21] P. J. Dagnall *et al.*, J. Phys. G **19**, 465 (1993).
[22] R. M. Clark *et al.*, Nucl. Phys. **A562**, 121 (1993).
[23] Y. LeCoz *et al.*, Z. Phys. A **348**, 87 (1994).
[24] P. J. Dagnall *et al.*, J. Phys. G **20**, 1591 (1994).
[25] M. G. Porquet *et al.*, J. Phys. G **20**, 765 (1994).
[26] N. Fotiades *et al.*, J. Phys. G **21**, 911 (1995).
[27] N. Fotiades *et al.*, Z. Phys. A **354**, 169 (1996).
[28] R. M. Clark *et al.*, Phys. Rev. Lett. **78**, 1868 (1997).
[29] S. Chmel, F. Brandolini, R. V. Ribas, G. Baldsiefen, A. Görgen, M. De Poli, P. Pavan, and H. Hübel, Phys. Rev. Lett. **79**, 2002 (1997).
[30] S. Frauendorf, Nucl. Phys. **A557**, 259c (1993); (private communication).
[31] J. R. Hughes *et al.*, Phys. Rev. C **51**, R447 (1995); L. P. Farris *et al.*, *ibid.* **51**, R2288 (1995).
[32] A. M. Baxter *et al.*, ANU Annual Report, 1995, p. 29; ANU Annual Report, 1996, p. 30; Abstracts of Conference on Nuclear Structure Studies at the Limits, 1996, p. 111.
[33] N. Fotiades *et al.*, Z. Phys. A **359**, 7 (1997).
[34] D. P. McNabb *et al.*, Phys. Rev. C **56**, 2474 (1997).
[35] R. B. Firestone, V. S. Shirley, C. M. Baglin, S. Y. Frank Chu, and J. Zipkin, *Table of Isotopes* (Wiley, New York, 1996), and references therein.
[36] H Hübel, A. P. Byrne, S. Ogaza, A. E. Stuchbery, G. D. Dracoulis, and M. Guttormsen, Nucl. Phys. **A453**, 316 (1986), and references therein.
[37] S. Frauendorf, J. Reif, and G. Winter, Nucl. Phys. **A601**, 41 (1996).
[38] S. Frauendorf, Z. Phys. A **358**, 163 (1997).